Exosomes derived from bone marrow mesenchymal stem cells inhibit neuroinflammation after traumatic brain injury

https://doi.org/10.4103/1673-5374.339489

Date of submission: July 24, 2021

Date of decision: November 25, 2021

Date of acceptance: January 19, 2022

Date of web publication: April 29, 2022

Liang Wen[1, #], Ya-Dong Wang[1, *, #], Dong-Feng Shen[2], Pei-Dong Zheng[1], Meng-Di Tu[1], Wen-Dong You[1], Yuan-Run Zhu[1], Hao Wang[1], Jun-Feng Feng[3], Xiao-Feng Yang[1, *]

From the Contents

Graphical Abstract *microRNAs in neuroprotection after traumatic brain injury (TBI)*

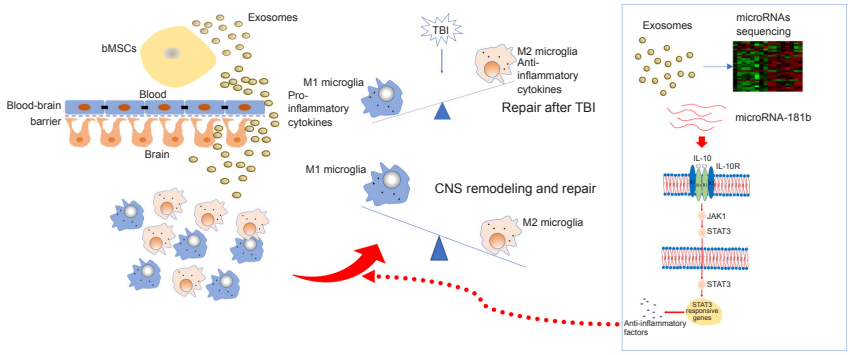

Abstract

Exosomes derived from bone marrow mesenchymal stem cells can inhibit neuroinflammation through regulating microglial phenotypes and promoting nerve injury repair. However, the underlying molecular mechanism remains unclear. In this study, we investigated the mechanism by which exosomes derived from bone marrow mesenchymal stem cells inhibit neuroinflammation. Our *in vitro* co-culture experiments showed that bone marrow mesenchymal stem cells and their exosomes promoted the polarization of activated BV2 microglia to their anti-inflammatory phenotype, inhibited the expression of proinflammatory cytokines, and increased the expression of anti-inflammatory cytokines. Our *in vivo* experiments showed that tail vein injection of exosomes reduced cell apoptosis in cortical tissue of mouse models of traumatic brain injury, inhibited neuroinflammation, and promoted the transformation of microglia to the anti-inflammatory phenotype. We screened some microRNAs related to neuroinflammation using microRNA sequencing and found that microRNA-181b seemed to be actively involved in the process. Finally, we regulated the expression of miR181b in the brain tissue of mouse models of traumatic brain injury using lentiviral transfection. We found that miR181b overexpression effectively reduced apoptosis and neuroinflamatory response after traumatic brain injury and promoted the transformation of microglia to the anti-inflammatory phenotype. The interleukin 10/STAT3 pathway was activated during this process. These findings suggest that the inhibitory effects of exosomes derived from bone marrow mesenchymal stem cells on neuroinflamation after traumatic brain injury may be realized by the action of miR181b on the interleukin 10/STAT3 pathway.

Key Words: apoptosis; bone marrow mesenchymal stem cells; BV2 microglia; exosome; interleukin 10; lentiviral transfection; microRNA-181b; neuroinflammation; phenotype; signal transducer and activator of transcription 3; traumatic brain injury

Introduction

Microglia are the resident macrophages of the nervous system (Arslan et al., 2013). They are responsible for regulating the microenvironment of the nervous system, phagocytosis of extracellular debris, and initiation of inflammation. Therefore, they are considered to be basic immune cells in the central nervous system that regulate immune responses and brain function (Hansson and Rönnbäck, 2003). Microglia have two phenotypes after traumatic brain injury (TBI): either the "classically activated" M1 phenotype or "alternatively activated" M2 phenotype. The balance between classically and alternatively activated microglial phenotypes was associated with the prognosis of central nervous system diseases (Qin et al., 2018). The M1 phenotype exhibits pro-inflammatory responses and expresses pro-inflammatory cytokines. In contrast, the M2 type exhibits anti-inflammatory effects and produces anti-inflammatory factors. However, there is no absolute boundary between them. There are cells that exhibit markers of both the M1 and M2 phenotypes. Nonetheless, researchers believe that demonstrating the complex phenotype of microglia in the central nervous system based on the M1/M2 classification is quite controversial because the two phenotypes exist upon stimulation and may thus revert to the other phenotype. It is a reversible process of modification. Transformation of phenotype and function may be a process with temporal and spatial heterogeneity (Stout and Suttles, 2004; Kigerl et al., 2009; Kumar and Loane, 2012).

In the wave of stem cell research at the beginning of the 21st century, mesenchymal stem cells (MSCs) from various tissues were used to treat nerve damage after brain injury or cerebral ischemia. Cells and their exosomes have shown some neurorestorative effects for neurological diseases and injury in preclinical and clinical studies (Shevela et al., 2019; Huang et al., 2020). Bone marrow mesenchymal stem cells (bMSCs) are capable of repairing and replacing damaged tissues by differentiating into effector cells, such as neurons and glial cells (Hermann et al., 2004; Wislet-Gendebien et al., 2005; Pirzad Jahromi et al., 2015; Zhao et al., 2015; Fesharaki et al., 2018; Wood et al., 2018). They can also secrete some cytokines to inhibit neuroinflammation and promote nerve repair. Thus, MSCs were considered to be a promising method for treating diseases affecting the central nervous system. Researchers have found that the role of repair is through paracrine effects and the exosomes secreted by MSCs rather than cell replacement

[1]The First Affiliated Hospital, School of Medicine, Zhejiang University, Hangzhou, Zhejiang Province, China; [2]Department of Intensive Care Unit, The First Hospital of Jiaxing, Jiaxing, Zhejiang Province, China; [3]Department of Neurosurgery, Renji Hospital, School of Medicine, Shanghai Jiao Tong University, Shanghai, China

***Correspondence to:** Xiao-Feng Yang, MD, zjcswk@zju.edu.cn; Ya-Dong Wang, MD, 11718340@zju.edu.cn.

https://orcid.org/0000-0003-0994-5118 (Xiao-Feng Yang); https://orcid.org/0000-0002-0981-7717 (Ya-Dong Wang)

#Both authors contributed equally to this work.

Funding: *This work was supported by the National Natural Science Foundation of China, Nos. 81971159 (to LW), 81771317 (to JFF).*

How to cite this article: *Wen L, Wang YD, Shen DF, Zheng PD, Tu MD, You WD, Zhu YR, Wang H, Feng JF, Yang XF (2022) Exosomes derived from bone marrow mesenchymal stem cells inhibit neuroinflammation after traumatic brain injury. Neural Regen Res 17(12):2717-2724.*

(Lai et al., 2010; Reis et al., 2012; van Koppen et al., 2012; Arslan et al., 2013; Bian et al., 2014; Tian et al., 2018). Exosomes are membranous vesicles secreted by different cells and are capable of crossing the blood-brain barrier (Zhuang et al., 2011). They play a major role in cell-cell interactions. Exosomes contain many components such as proteins, lipids, and nucleic acids. MicroRNAs contained in exosome vesicles have been found to play important roles in many physiological and pathological processes (Timmers et al., 2007; Reis et al., 2012; Arslan et al., 2013; Xin et al., 2013; Bian et al., 2014; Shao et al., 2017). Exosomes have been previously reported to display neuroprotective effects in rats after TBI (Kim et al., 2016). Some scholars have suggested that exosomes derived from MSCs can inhibit neuroinflammation and promote neural repair by regulating microglial phenotypes (Li et al., 2017; Xu et al., 2017). However, the molecular mechanisms involved have not been reported. Moreover, there is still no conclusion regarding the mechanism involved during exosome regulation of the microglial phenotype after TBI. As such, this study hypothesized that bMSC-derived microRNAs in exosomes exhibit neuroprotective effects. *In vivo* and *in vitro* experiments and microRNA sequencing was conducted to explore the microRNAs involved in neuroprotection. Lentivirus was subsequently used to regulate the expression levels of related microRNAs to test the hypothesis and verify the possible downstream mechanisms.

Materials and Methods

All animal experiments were approved by the Animal Ethics Committee of the First Affiliated Hospital, School of Medicine, Zhejiang University (Reference No. 201991) on February 13, 2019 and followed the National Institutes of Health guide for the Care and Use of Laboratory Animals.

Culturing and identification of BV2 cells and bMSCs

BV2 cells (RRID: CVCL_0182) were provided by the Institute of Neuroscience, School of Medicine, Zhejiang University. The BV2 cells were cultured in Dulbecco's modified Eagle medium high glucose culture medium (Hyclone, Logan, UT, USA) supplemented with 10% fetal bovine serum (Gibco, Melbourne, Australia). BV2 cells were activated using lipopolysaccharide (1000 ng/mL; Sigma-Aldrich, St. Louis, MO, USA) at 37°C for 48 hours. bMSCs were derived from tibia and femur bone marrow from male C57BL/6J mice (n = 5, specific-pathogen-free, aged 6–8 weeks and weighing 18–20 g; Experimental Animal Center of Zhejiang Province, Zhejiang, China; license No. SCXK (Zhe) 2014-0001). The tibia and femur of mice were immediately harvested and immersed in 75% alcohol for 15 minutes after being sacrificed by dislocating the cervical vertebrae under ketamine anesthesia. The epiphyses of each side of the femur and tibia bone were cut. Femur and tibia bone marrow was flushed with Roswell Park Memorial Institute medium 1640 (Hyclone) and collected into 10 mL culture dish with 10% fetal bovine serum. They were cultured at 37°C in a 5% CO_2 environment. Half of the volume of culture medium was changed after 48 hours. The medium was then changed every 3 days for a further 15–21 days. Cell passage was performed when cell confluence reached approximately 80%. Cultured bMSCs between passages 3 and 5 were used for the following experiments. BV2 cells and bMSCs were subsequently identified through immunostaining using anti-ionized calcium binding adapter molecule 1 (Iba1) and anti-CD44 antibodies, respectively.

Extraction and identification of exosomes

Exosomes were extracted from the cell culture supernatant of bMSCs. The bMSCs were first washed twice with phosphate-buffered saline (Servicebio, Wuhan, China). The culture medium was then replaced with exosome depleted fetal bovine serum (System Biosciences, Palo Alto, CA, USA) for another 48 hours. The resultant supernatant was collected and first centrifuged for 10 minutes at 300 × g. It was then transferred to an ultracentrifuge (Hitachi Limited, Tokyo, Japan, Himac cp80wx) and centrifuged for 30 minutes at 10,000 × g. Further centrifugation of the supernatant was performed at 100,000 × g for 70 minutes to form an exosome pellet. The supernatant was discarded, and the pellet was resuspended in 500 µL phosphate-buffered saline for use in subsequent experiments. The exosomes were then identified using a transmission electron microscope (FEI, Hillsboro, OR, USA). Nanoparticle tracking analysis was performed using ZetaVIEW 8.04 (Particle Metrix, Meerbusch, Germany) to measure the diameter and particle number of the exosomes. Two protein samples from exosomes with different concentrations were prepared. The antibodies of exosome marker tumor susceptibility gene 101 (TSG101; Abcam, Cambridge, UK) and heat shock protein 70 (HSP70; Biolegend, San Diego, CA, USA) were detected using western blot assay.

In vitro co-culture experimental design

BV2 cells were first kept at 37 °C and activated using lipopolysaccharide for 48 hours. The upper inserts of Transwell chamber (0.4 µm pore size, Corning Life Sciences, Corning, NY, USA) were filled with Dulbecco's modified Eagle medium (500 µL/well) and seeded with bMSCs (0.5×10^5 cells/well) or exosomes derived from bMSCs (6.3×10^9 particles/well). The lower chambers were seeded with activated BV2 cells (2×10^5 cells/well). Cell-climbing slices were set in the lower chambers in advance. The Transwell plates were incubated for 48 hours in an incubator set at 37°C and 5% CO_2. The total RNA of BV2 cells was extracted, and the cell-climbing slices were harvested for further analysis. The BV2 cells in the microglia (MG) group served as a negative control. BV2 cells from the co-culture system were used in flow cytometry, immunofluorescence, and quantitative polymerase chain reaction. The *in vitro* experiments were repeated three times with five samples for each group.

Cell phenotype analysis

BV2 cells in the lower chambers were collected after 48 hours of co-culturing for flow cytometry analysis. To verify the percentage of M1 and M2 macrophages, the cells were incubated with the following mixture of directly conjugated antibodies: fluorescein isothiocyanate-conjugated anti-Iba1 antibodies, allophycocyanin-conjugated anti-CD86 antibodies, and phycoerythrin-conjugated anti-CD206 antibodies. They were then fixed with 1000 µL phosphate-buffered saline for 30 minutes at room temperature (25°C) followed by determination of the proportions of $Iba1^+CD86^+CD206^-$ (M1 phenotype) and $Iba1^+CD86^-CD206^+$ (M2 phenotype) BV2 microglia. BV2 cells were evaluated using a flow cytometer (BD FACSCanto™ II Flow cytometer; BD Biosciences, San José, CA, USA) and FlowJo v10.4 software (FlowJo, LLC, Ashland, OR, USA). Six samples were detected per group.

MicroRNA sequencing

After culturing in exosome-depleted fetal bovine serum for 48 hours, the total RNA from bMSCs and exosomes derived from bMSCs were collected for the following experiment. MicroRNA sequencing was performed to compare microRNA expression levels between bMSCs and exosomes derived from bMSCs. The sequencing process included the following steps: 1) total RNA collection, 2) 3′ and 5′ adapter ligation, 3) real-time polymerase chain reaction amplification, 4) small RNA library gel purification, and 5) library validation. The microRNA data was analyzed using ACGT101-miR (LC Sciences, Houston, Texas, USA). The analysis process was as follows: 1) 3′ connector and non-specific sequences were removed, 2) the length of sequences was maintained between 18–26 nt through length screening, 3) mRNAs were used for comparative analysis and the filtration of remaining sequences, 4) filtering was used to obtain effective data and for microRNA identification, and 5) differentially expressed microRNAs were analyzed. A P-value ≤ 0.05 was considered statistically significant. The microRNAs sequencing and data analysis were performed by OBiO Technology (Shanghai) Corp., Ltd. (Shanghai, China).

In vivo animal experimental design

Healthy C57BL/6J male mice (n = 100, specific-pathogen-free, aged 6–8 weeks and weighing 18–20 g) were purchased from the Experimental Animal Center of Zhejiang Province (Zhejiang, China; certificate No. SCXK (Zhe) 2014-0001). The *in vivo* experiment was divided into two parts.

In the first part, C57BL/6J mice were randomly divided into four groups (n = 5/group): sham (sham operation), brain trauma (TBI), normal saline (200 µL normal saline was injected through the tail vein after TBI, TBI + saline), and exosome groups (200 µL exosomes (6.3×10^{10} particles/mL) were injected through the tail vein after TBI, TBI + Exo). The normal saline and exosomes were daily injected until the mice were sacrificed at 1, 3, or 7 days post-TBI.

In the second part, mice were randomly divided into three groups (n = 5/group): TBI (TBI in normal mice), TBI-down (TBI in microRNA downregulated mice), and TBI-up groups (TBI in microRNA upregulated mice).

TBI model

A TBI model was induced as described in our previous study (Wen et al., 2019). A scalp incision was first made to expose the skull. A cranial window (3-mm diameter) was then drilled in the right parietal area of the skull, 2 mm away from the midline. A lateral fluid percussion injury device (Virginia Commonwealth University Biomedical Engineering, Richmond, VA, USA) was used to induce TBI. Mice were anesthetized with an intraperitoneal injection of ketamine (80–100 mg/kg; Sigma). The device was tested by delivering approximately 10 pulses until a steady signal was produced. The angle of the pendulum starting position was adjusted to reach a pulse intensity of approximately 2.0 atm.

Lentiviral transfection

MiR-181b inhibitor lentivirus and miR-181b-overexpressing lentivirus were purchased from Jikai Gene (Jikai Gene Chemical Technology Co., Ltd., Shanghai, China). The lentiviruses were injected into the exposed cortex of each mouse (1 µL per mouse) through the cranial window using a stereotaxic instrument and a microinjection pump (RWD Life Science, Shenzhen, China) 7 days before TBI. Infectious lentiviruses were used to up- or downregulate the expression level of microRNA-181b. The expression level of microRNA-181b in the cerebral cortex was tested by real-time quantitative polymerase chain reaction 7 days after the transfection.

Tissue preparation

The C57BL/6J mice were injected intraperitoneally with ketamine (80–100 mg/kg) for anesthesia, and then sacrificed using 3 L/min CO_2 asphyxiation and brains were removed following decapitation. The brain tissues were harvested and excised on ice on days 1, 3, and 7 post-initiation of brain trauma. Total RNA and proteins of the brain tissues were extracted for follow-up real-time quantitative polymerase chain reaction and western blot assay. Brain tissues harvested on day 7 post-initiation of TBI were prepared into sections for TdT-mediated dUTP nick-end labeling (TUNEL) staining and immunofluorescence analysis. The *in vivo* experiments were performed twice with five biological replicates per group.

Immunofluorescence analysis

Immunofluorescence analysis was performed based on the classical protocol. Anti-Iba1 (mouse, 1:500, Abcam, Cat# ab15690, RRID: AB_2224403) and anti-CD44 (rabbit, 1:500, Proteintech, Cat# 15675-1-AP, RRID: AB_2076198) were used to identify BV2 cells and bMSCs, respectively. The cell climbing slices in the *in vitro* experiments were double stained with anti-arginase-1 (Arg1;

rabbit, 1:1000, Proteintech, Cat# 16001-1-AP, RRID: AB_2289842) and anti-inducible nitric oxide synthase (iNOS; mouse, 1:500, Santa Cruz Biotechnology, Santa Cruz, CA, USA, Cat# sc-7271 AF546, RRID: AB_2891105) followed by 4',6-diamidino-2-phenylindole (DAPI) staining. Brain tissues collected in the first part of the animal experiments were prepared into sections and stained with anti-Arg1 and DAPI. All primary antibodies were applied sequentially with overnight incubations at 4°C. CoraLite594 donkey anti-rabbit IgG (1:500, Proteintech, Cat# SA00013-8, RRID: AB_2857367), CoraLite488 donkey anti-rabbit IgG (1:500, Proteintech, Cat# SA00013-6, RRID: AB_2890972), and CoraLite488 donkey anti-mouse IgG (1:500, Proteintech, Cat# SA00013-5, RRID: AB_2890971) were used as secondary antibodies. The secondary antibodies were incubated for 30 minutes at room temperature in the dark. Evaluation of the cell-climbing slices and brain sections was performed using a confocal microscope (Olympus, Melville, NY, USA). Data were analyzed by counting the number of Iba1-, CD44-, or Arg1-positive cells in the two randomly selected high-magnification (200× or 400×) fields in each cell climbing slice or brain section.

Real-time polymerase chain reaction

The mRNA expression levels of inflammatory factors, such as interleukin-1beta (IL-1β), interleukin-6 (IL-6), tumor necrosis factor-α (TNF-α), interleukin-10 (IL-10), and transforming growth factor-β (TGF-β), were quantified using real-time polymerase chain reaction to determine whether exosomes and micro181b could inhibit neuroinflammation. BV2 cells were collected 48 hours after the coculture experiments. The expression factors were quantified to verify the effect of bMSCs and exosomes derived from bMSCs. The factors were quantified on day 1, 3, and 7 post-TBI in the *in vivo* experiment. This was done to observe the dynamic changes in related factors in both parts of the animal experiments. Moreover, the expression levels of candidate microRNAs selected and key proteins of inflammatory signaling pathway (nuclear factor-kappa B, NFκB; activator of transcription 3, STAT3) were quantified as well.

Total RNA from BV2 cells and brain tissues of mice from all groups were extracted using an RNA purification kit (EZBioscience, Roseville, MN, USA) in accordance with the manufacturer's instructions. The concentration of RNA samples was measured using a Nanodrop® spectrophotometer (Thermo Scientific, Wilmington, DE, USA), and the samples were stored at −80°C for preservation. First-strand cDNA synthesis was performed using normal reverse transcription for mRNA analysis. A 4× EZscript Reverse Transcription Mix II (EZBioscience, Roseville, MN, USA) was used in this process. A poly(A) tail was added to the microRNAs followed by reverse transcription for microRNA analysis. All primers were synthesized by Sangon Biotech Co., Ltd. (Shanghai, China). The primer sequences are listed in **Tables 1** and **2**. U6 was used as the internal reference gene to determine microRNA expression while glyceraldehyde-3-phosphate dehydrogenase served as the internal reference gene for expression of other genes. Gene expression levels were calculated using the comparative CT (ΔΔCT). Three samples were provided for each group, and every real-time quantitative polymerase chain reaction experiment was repeated twice.

Table 1 | **Primer sequences of several mRNAs**

Primer	Sequence (5'–3')
GAPDH	Forward: TGG ATT TGG ACG CAT TGG TC
	Reverse: TTT GCA CTG GTA CGT GTT GAT
IL-1β	Forward: GCA ACT GTT CCT GAA CTC AA CT
	Reverse: ATC TTT TGG GGT CCG TCA ACT
IL-6	Forward: TAG TCC TTC CTA CCC CAA TTT CC
	Reverse: TTG GTC CTT AGC CAC TCC TTC
TNF-α	Forward: GCA GGA GGG ACT TCA GGT GA
	Reverse: GCC CCC ACT GTC CGT TCT
IL-10	Forward: CGG CTG AGG CGC TGT
	Reverse: TGC CTT GCT CTT ATT TTC ACA GG
TGF-β	Forward: TCT GCA TTG CAC TTA TGC TGA
	Reverse: AAA GGG CGA TCT AGT GAT GGA
NF-κB	Forward: ATG GCA GAC GAT GAT CCC TAC
	Reverse: TGT TGA CAG TGG TAT TTC TGG TG
STAT3	Forward: CAA TAC CAT TGA CCT GCC GAT
	Reverse: GAG CGA CTC AAA CTG CCC T

GAPDH: Glyceraldehyde-3-phosphate dehydrogenase; IL: interleukin; NF-κB: nuclear factor kappa-B; STAT3: signal transducer and activator of transcription 3; TGF-β: transforming growth factor-β; TNF-α: tumor necrosis factor-α.

Table 2 | **Primer sequences of some microRNAs**

microRNA	Sequence (5'–3')
U6	Forward: AGA GAA GAT TAG CAT GGC CCC TG
mmu-let-7c	Forward: GCG TGA GGT AGT AGG TTG TAT GGT T
mmu-miR-124	Forward: TAA GGC ACG CGG TGA ATG C
mmu-miR-21a	Forward: CGG GTA GCT TAT CAG ACT GAT GTT GA
mmu-miR-181b	Forward: AAC ATT CAT TGC TGT CGG TGG G
Universal reverse primer	Reverse: ATC CAG TGC AGG GTC CGA GG

TdT-mediated dUTP nick-end labeling assay

TUNEL assay was done in the two *in vivo* experiments to determine whether bMSCs-Exo and different expression levels of microRNA-181b would influence apoptosis in the damaged cerebral cortex at 7 days post-TBI. TUNEL staining was performed using a TUNEL kit (Biyuntian Biotechnology Co., Ltd., Shanghai, China) in accordance with the manufacturer's instructions. The number of TUNEL-positive cells in two high-magnification fields (400×) of each brain section was counted to evaluate the effect of exosomes or microRNA-181b. The TUNEL assay was performed twice.

Western blot analysis

The expression level of iNOS and Arg1 were verified using WB analyses to determine the expression of iNOS positive cells (M1) and Arg1 positive cells (M2), respectively, in the *in vivo* experiments. The expression level of signal transducer and activator of transcription 3 (STAT3), a potential responsible pathway, was measured to verify its effect in the second part of the animal experiments. Protein extracts were obtained from the brain tissue samples on day 7 post-TBI and their concentration determined using a bicinchoninic acid kit (Biyuntian Biotechnology Co., Ltd.). The primary antibody anti-Arg1 was used at 1:1000 dilution, anti-iNOS (mouse, Santa Cruz Biotechnology, Cat# sc-7271 AF546, RRID: AB_2891105) at 1:500 dilution, anti-STAT3 (mouse, Santa Cruz Biotechnology, Cat# sc-8019, RRID: AB_628293) at 1:200 dilution, anti-α-tubulin (rabbit, Invitrogen, Cat# PA5-19489, RRID: AB_10984311) at 1:500, and anti-β-actin (rabbit, Abcam, Cat# ab8227, RRID: AB_2305186) at 1:500 dilution in the western blot assay. The blots were incubated with the primary antibody at 4°C overnight on a shaker. The following secondary antibodies were used: horseradish peroxidase-conjugated goat anti-mouse (1:10,000, Biosharp, Guangzhou, China, Cat# BL001A, RRID: AB_2827665), horseradish peroxidase-conjugated goat anti-rabbit (1:10,000, Biosharp, Cat# BL003A, RRID: AB_2827666). Horseradish peroxidase-conjugated secondary antibodies were incubated with polyvinylidene fluoride membranes (Millipore, Bedford, MA, USA) for 30 minutes at room temperature. Protein expression relative to the internal reference was detected using ImageJ software (v1.52a, National Institutes of Health, Bethesda, MD, USA) to compare optical densities. This process was performed twice.

Statistical analysis

No statistical methods were used to predetermine sample size for animal experiments. The selection of sample size for animal experiments was carried out in preliminary experiments, as well as by examining similar studies (Zhuang et al., 2011; Xin et al., 2013). The evaluator was blinded to grouping. Statistical Product and Service Solutions (SPSS, Version 17.0, SPSS, Chicago, IL, USA) was used to perform data analyses. Data are reported as mean ± standard deviation (SD). Variations between groups were calculated using one-way analysis of variance. In addition, the least significant difference test was employed for group comparisons. *P*-values less than 0.05 indicated a significant difference between groups.

Results

bMSCs and their derived exosomes induce the transformation of microglial polarization towards the anti-inflammatory phenotype

Exosomes were isolated from bMSCs using ultracentrifugation and identified using transmission electron microscopy, nanoparticle tracking analysis, and western blot analysis. A typical cup-shaped membrane vesicle morphology was observed (**Figure 1**). The size distribution profiles from the nanoparticle tracking analysis revealed that most vesicles had a diameter of ~130 nm. The original concentration of exosomes was 6.3×10^{10} particles/mL (exosomes detected were diluted by 1000-fold). Western blotting analysis further revealed that exosome markers TSG101 and HSP70 were expressed in the exosomes (**Figure 1**).

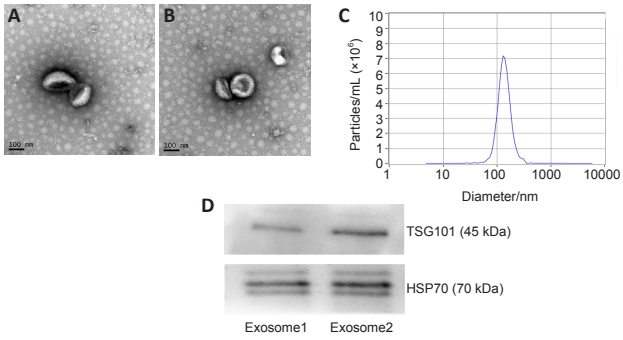

Figure 1 | **Identification of exosomes derived from bone marrow mesenchymal stem cells.**

(A, B) Transmission electron microscopy revealed the membrane vesicle had a typical cup-shaped morphology. Scale bars: 100 nm. (C) Nanoparticle tracking analysis revealed that most vesicles had a diameter of approximately 130 nm. The original concentration of the exosomes was 6.3×10^{10} particles/mL. (D) Western blot assay further revealed that the exosome markers, TSG101 and HSP70, were expressed in the exosomes. HSP70: Heat shock protein 70; TSG101: tumor susceptibility gene 101.

After BV2 microglia cells were activated, they were then co-cultured with bMSCs or exosomes for 48 hours to facilitate the polarization of activated BV2 cells toward the anti-inflammation type (**Figure 2A**). This was performed

to investigate the effects of bMSCs and bMSC-derived exosomes on the polarization phenotypes of activated BV2 cells in a co-culture system. The expression of the anti-inflammation marker, Arg1, was increased significantly in the MG + bMSCs and MG + Exo groups, and the expression of pro-inflammation marker iNOS was decreased in the MG + bMSCs and MG + Exo groups. Flow cytometry analysis was then performed to determine the proportion of pro-inflammatory and anti-inflammatory phenotype cells (**Figure 2B**). Activated BV2 cells were transformed to the anti-inflammatory phenotype after 48 hours of co-culturing with bMSCs or exosomes. Moreover, the exosomes were associated with a stronger anti-inflammatory effect (**Figure 2C**).

bMSCs and their derived exosomes promote the expression of anti-inflammatory factors

Real-time quantitative polymerase chain reaction was used to detect the mRNA expression of BV2 cell-related inflammatory factors after 48 hours of co-culture with bMSCs or exosomes. Both bMSCs and exosomes inhibited the mRNA expression of pro-inflammatory factors (IL-1β, IL-6, and TNF-α), but promoted the mRNA expression of anti-inflammatory factors (IL-10 and TGF-β) (**Figure 3**).

Exosomes decrease apoptosis in injured cerebral cortex of TBI mice

The lesion area and apoptotic cerebral cortical cells were determined 7 days after TBI to detect the effects of exosomes on the nervous system post-TBI *in vivo* (**Figure 4**). The damaged area in mice in the TBI + Exo group was smaller than that in the TBI and TBI + saline groups (**Figure 4A** and **B**). Brain sections were then subjected to TUNEL staining followed by quantification of TUNEL-positive cells. The TBI + Exo group had significantly fewer apoptotic neurons than did the TBI and TBI + saline groups (**Figure 4C** and **D**).

Exosomes inhibit inflammation of the brain tissue after TBI

An *in vivo* experiment was designed in which exosomes were injected through the tail vein followed by induction of the TBI model to examine whether exosomes could inhibit inflammation in the central nervous system after induction of TBI. The expression levels of Arg1, iNOS, and inflammatory factors were then detected using immunofluorescence, western blot, and real-time quantitative polymerase chain reaction (**Figure 5**). The proportion of Arg1-positive cells in the TBI + Exo group was significantly higher than that in the other groups (**Figures 5A** and **B**). In the same line, according to the western blot results, the protein expression level of Arg1 in the TBI + Exo group was significantly higher than that in the other groups. However, the expression of iNOS protein in the TBI + Exo group was significantly lower than that in the TBI and TBI + saline group ($P < 0.05$; **Figure 5C**). **Figure 5DI–III** shows the mRNA expression levels of the related inflammatory factors 1, 3, and 7 days, respectively, after the onset of TBI. Evidently, the mRNA expression levels of IL-10 and TGF-β in the TBI + Exo group were higher than those in the TBI and TBI + saline groups on days 1, 3, and 7 post-TBI. Moreover, the mRNA expression levels of IL-1β and TNF-α in the TBI + Exo group were lower than those in the TBI and TBI + saline groups on days 3 and 7 post-TBI. Injection of exosomes upregulated the expression of STAT3 but inhibited the expression of nuclear factor-kappa B (NFκB) 7 days post-TBI (**Figure 5D [IV]**).

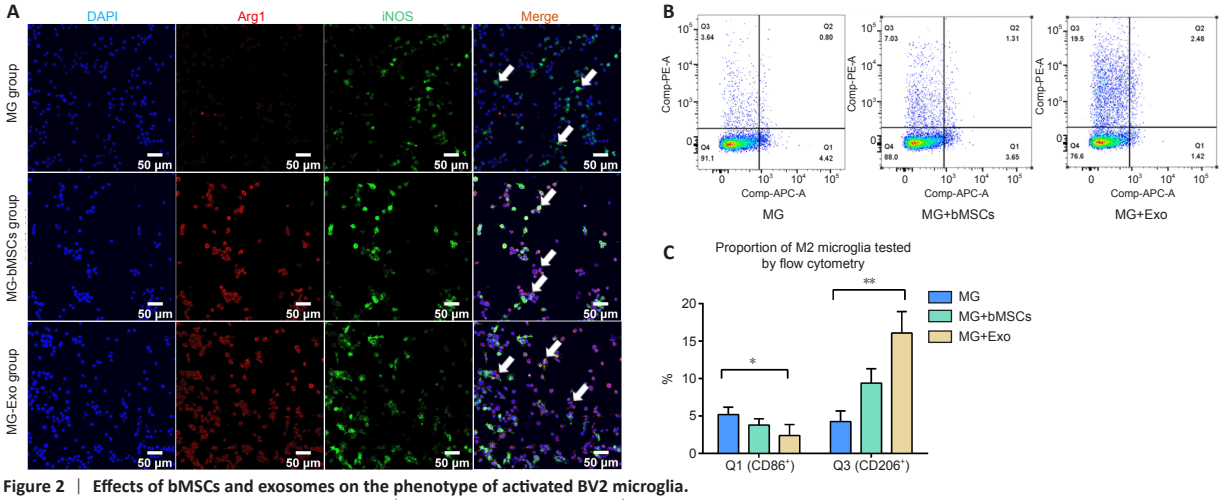

Figure 2 | **Effects of bMSCs and exosomes on the phenotype of activated BV2 microglia.**
(A) Immunofluorescence results of DAPI (blue), Arg1+ (CoraLite 594, red), and iNOS+ (Coralite 488, green) cells. Compared with the MG group, there were significantly more Arg1/iNOS double-positive cells (arrows) in the MG + bMSCs and MG + Exo groups. Scale bars: 50 μm. (B, C) Flow cytometry analysis of the proportion of Iba1/CD86 double-positive and Iba1/CD206 double-positive cells. The proportion of CD206/Iba-1 double-positive (Q3) cells in the MG + Exo group was significantly higher than in the MG and MG + bMSCs groups. However, the number of CD86/Iba-1 double-positive (Q1) cells in the MG + Exo group was significantly lower than that in the MG group. Data are expressed as mean ± SD. Experiments were repeated three times with five samples in each group. *$P < 0.05$, **$P < 0.05$ (one-way analysis of variance followed by the least significant difference test). Arg1: Arginase-1; DAPI: 4′,6-diamidino-2-phenylindole; iNOS: inducible nitric oxide synthase.

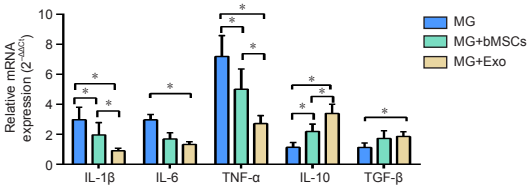

Figure 3 | **mRNA expression for inflammatory factors in BV2 cells in the co-culture system after 48 hours.**
Data are expressed as mean ± SD. The experiments were repeated three times with five samples in each group. *$P < 0.05$ (one-way analysis of variance followed by least significant difference *t*-test). IL: Interleukin; TGF-β: transforming growth factor-β; TNF-α: tumor necrosis factor-α.

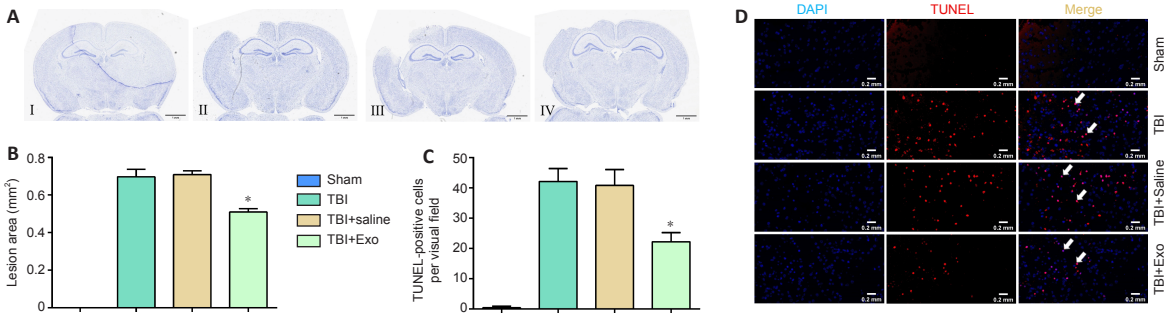

Figure 4 | **Exosomes induce reduction of the injured area and cerebral cell apoptosis in the lesion areas of TBI mice.**
(A) Nissl staining of the sham (I), TBI (II), TBI + saline (III), and TBI + Exo (IV) groups. The injured area in TBI + Exo group was significantly lower than that in TBI and TBI + saline groups. (B) Quantification of lesion areas. (C) Quantification of TUNEL-positive cells. Compared with TBI and TBI + saline groups, the number of apoptotic cells in the TBI + Exo group was markedly lower. Data are expressed as mean ± SD. The quantification was performed with five high-magnification fields (400×) in each group. *$P < 0.05$, *vs.* TBI and TBI + saline groups (one-way analysis of variance followed by the least significant difference test). (D) TUNEL staining of sham, TBI, TBI + saline, and TBI + Exo groups. There were fewer apoptotic cells (TUNEL-positive cells, arrows) in the TBI + Exo group than in the TBI and TBI + saline groups. Red staining represents the TUNEL-positive cells (white arrows). Scale bars: 1 mm in A, 0.2 mm in D. DAPI: 4′,6-Diamidino-2-phenylindole; Exo: exosomes; TBI: traumatic brain injury; TUNEL: TdT-mediated dUTP nick-end labeling.

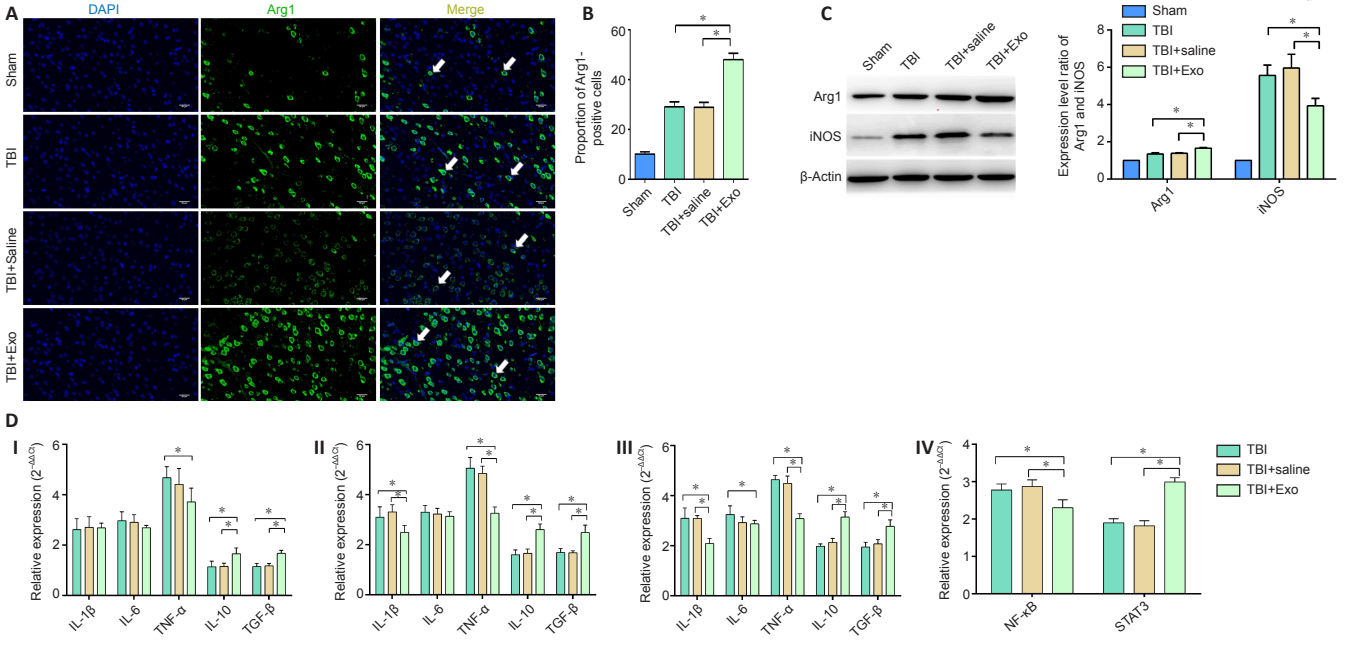

Figure 5 | **Effects of exosomes on neuroinflammation of injured area in TBI mice.**
(A) Immunofluorescence assay of Arg1 (CoraLite488, green) on brain slices 7 days post TBI. DAPI was stained as blue. TBI + Exo group showed more Arg1-positive cells (arrows) than any other groups. Scale bars: 200 μm. (B) Proportion of Arg1-positive cells. (C) Relative protein expression of Arg1 and iNOS using western blot assay. (D) mRNA expression levels of inflammatory factors on days 1 (I), 3 (II), and 7 (III) post-TBI and mRNA expression levels of NFκB and STAT3 on day 7 post-TBI (IV). The experiments were repeated twice with five samples in each group. Data are expressed as mean ± SD (n = 5 per group). *P < 0.05 (one-way analysis of variance followed by the least significant difference test). Arg1: Arginase-1; DAPI: 4′,6-diamidino-2-phenylindole; IL: interleukin; iNOS: inducible nitric oxide synthase; NF-κB: nuclear factor kappa-B; STAT3: signal transducer and activator of transcription 3; TBI: traumatic brain injury; TGF-β: transforming growth factor-β; TNF-α: tumor necrosis factor-α.

miRNA-181b is highly expressed in both bMSC exosomes and TBI brain tissues

microRNA sequencing of bMSCs and exosomes derived from bMSCs was performed to explore the effective components of exosomes. Sequencing results revealed that there were more than 500 microRNAs highly expressed and more than 300 microRNAs lowly expressed in the exosomes relative to their expression in bMSCs. The differentially expressed microRNAs are shown in the heatmap and volcano plot (**Figures 6A** and **B**). Based on microRNAs reported in other relevant studies (Ni et al., 2015; Harrison et al., 2016; Liu et al., 2018; Meng et al., 2019), let-7c, miR-124, miR-21a, and miR-181b were chosen to be intensively studied. The expression levels of these microRNAs in brain tissues of mice in the TBI + Exo group on day 7 post-TBI were determined. miR-181b was found to be highly expressed in the TBI + Exo group (**Figure 6C**). This strongly suggested that miR-181b plays a major role in inhibiting neuroinflammation and regulating the phenotype of microglia.

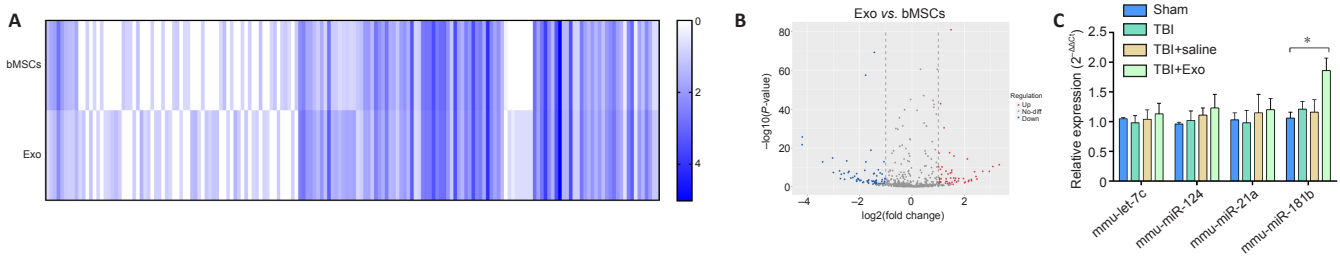

Figure 6 | **Differential expression of microRNAs between bMSCs and exosomes.**
(A) Heatmap of differentially expressed microRNAs between bMSCs and exosomes. The relative expression levels of hundreds of detected microRNAs were displayed in the heatmap. The intensity of the color indicates the expression of microRNAs, with a darker color meaning higher expression level. (B) Volcano plot of the differentially expressed microRNAs. Blue represents low expression while red denotes high expression in exosomes. Gray denotes lack of differences between them. (C) The differentially expressed microRNAs *in vivo*. Data are expressed as mean ± SD (n = 5 per group). *P < 0.05 (one-way analysis of variance followed by the least significant difference test). bMSCs: Bone marrow mesenchymal stem cells; Exo: exosome; mmu: musmusculus; TBI: traumatic brain injury.

Upregulation of microRNA-181b inhibits apoptosis of cortical cells, reduces neuroinflammation, and regulates the phenotype of microglia post TBI

Lentiviral vectors were used to obtain different expression levels of miR-181b to verify the role of miR-181b in the neuroinflammation process post-TBI. The expression level of miR-181b was detected 7 days after transfection of the mice with the lentivirus. Cell apoptosis detected in each group on day 7 post-TBI revealed that the number of TUNEL-positive cells in the miR-181b upregulation group was significantly lower than that in the other two groups (**Figures 7A** and **B**). The expression level of miR-181b in the upregulation and downregulation group was 2.7 times higher and 0.4 times lower than that in normal C57BL/6J mice, respectively (**Figure 7C**). The microglial markers, Arg1 and iNOS, and the transcriptional regulator, STAT3, were detected using western blot (**Figure 7D**). The TBI-up group had a higher expression level of Arg1 and STAT3, but a lower expression level of iNOS than did the normal and TBI-down groups. Inflammatory factors were also detected on day 1, 3, and 7 post-TBI (**Figure 7E [I–III]**). The mRNA expression level of IL-10 and TGF-β in the TBI-up group was significantly higher than that in the other two groups on day 1, 3, and 7 post-TBI (P < 0.05). However, the mRNA expression level of IL-1β in the TBI-up group was significantly lower than that in the other two groups on day 1, 3, and 7 post-TBI (P < 0.05). Similarly, the mRNA expression level of TNF-α in the TBI-up group was significantly lower than that in the other two groups on day 3 and 7 post-TBI (P < 0.05). Nonetheless, the expression level of IL-6 mRNA was not significantly different between groups on day 1, 3, and 7 post-TBI. Further analysis of the TBI-up group revealed that the expression levels of IL-10 and TGF-β mRNA gradually increased after TBI (**Figure 7E [IV]**).

Discussion

Microglia play an important role in regulating neuronal functions such as cell survival, neurogenesis, and neuroinflammation (Zhang and Fedoroff, 1996; Arnò et al., 2014; Ransohoff et al., 2015; Mosser et al., 2017). In healthy brain tissues, microglia can phagocytose cell debris and damaged neurons. Activated microglia can also release various pro-inflammatory and anti-inflammatory cytokines and mediators, such as interleukin-1β, interleukin-6, interleukin-10, arginase-1, cyclooxygenase-2, and inducible nitric oxide synthase among others (Kirkley et al., 2017; Pozzo et al., 2019).

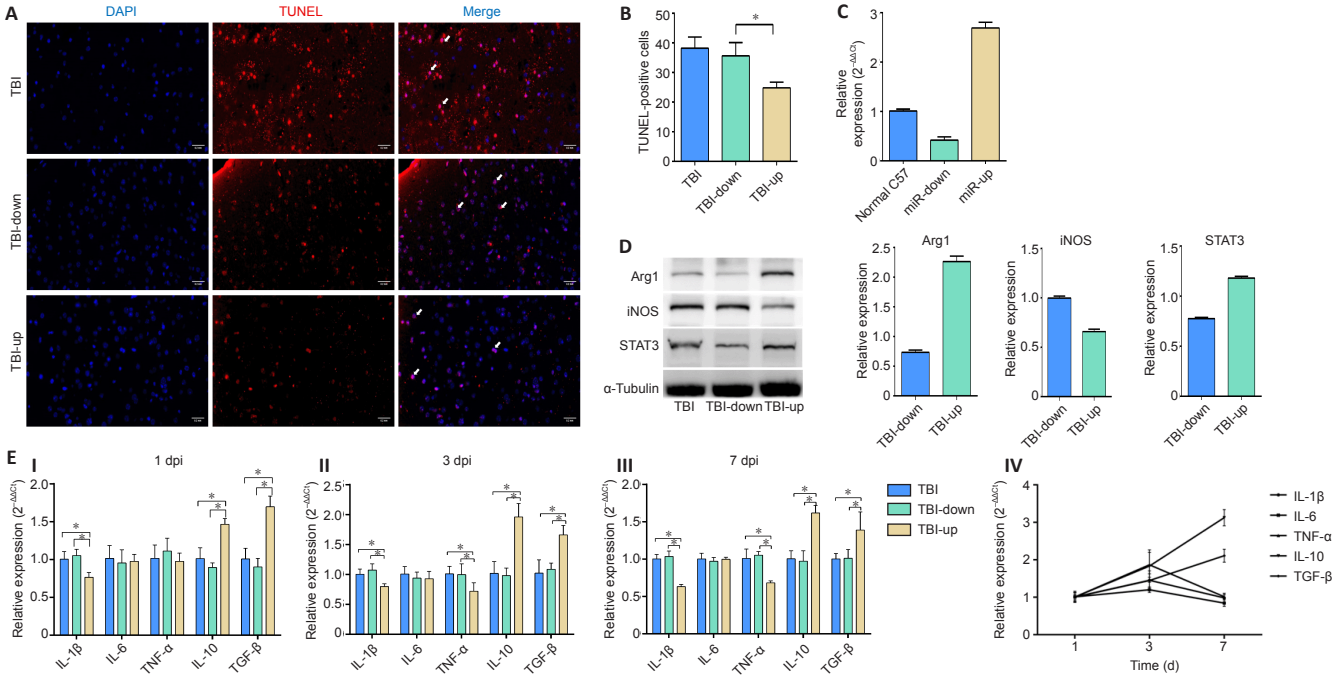

Figure 7 | **The effect of different expression levels of miR-181b on cerebral cell apoptosis and neuroinflammation in injured area of TBI mice.**
(A) TUNEL staining showing the levels of cerebral cell apoptosis (arrows) in the three groups. There were fewer apoptotic cells (TUNEL-positive cells) in the TBI-up group than in the other two groups. Scale bars: 0.2 mm. (B) Quantification of TUNEL-positive cells. (C) Expression level of miR-181b 7 days after the transfection with lentivirus. (D) Protein expression of microglia markers, Arg1 and iNOS, as well as the transcriptional regulator, STAT3. (E) mRNA expression of inflammatory factors on days 1, 3, and 7 post TBI (I–III). Dynamic changes in inflammatory factors in TBI-up group (IV). Data are expressed as mean ± SD (n = 5 per group). *P < 0.05 (one-way analysis of variance followed by the least significant difference test). Arg1: Arginase-1; DAPI: 4′,6-diamidino-2-phenylindole; Dpi: days post injury; IL: interleukin; iNOS: inducible nitric oxide synthase; STAT3: signal transducer and activator of transcription 3; TBI: traumatic brain injury; TGF-β: transforming growth factor-β; TNF-α: tumor necrosis factor-α.

Exosomes derived from MSCs protect various tissues from damage (Arslan et al., 2013; Tan et al., 2014; Zhu et al., 2014; Kim et al., 2016; Rager et al., 2016). Tian et al. (2018) conjugated c (RGDyk) to the surface of exosomes and then injected exosomes through the tail vein. Their results suggest a targeting delivery effect of exosomes after ischemia (Tian et al., 2018). Nonetheless, there are still many unanswered questions regarding their role in the pathophysiological process. Kim reported that exosomes isolated from MSCs could improve the cognitive impairment in TBI mice (Kim et al., 2016). However, the molecular signals that mediated interactions between exosomes and neurons to promote neuronal survival were still unclear.

Neuroinflammation affects the recovery of nerve function and the survival of neurons. As such, it is an important process in secondary brain injury. Herein, exosomes co-cultured with bMSCs inhibited the pro-inflammatory effect of activated microglia-like BV2 cells. They also played a crucial role in promoting macrophage polarization towards the M2 phenotype. Moreover, the BV2 cells expressed both Arg1 and iNOS at the same time. This result was consistent with other reports (Pettersen et al., 2011; Wong et al., 2011; Vogel et al., 2013). In the same line, Italiani reported that human macrophages could be polarized to the M1 phenotype and then mature to the M2 phenotype with continuous changes in culture conditions (Italiani et al., 2014). Similarly, after exposure to classic M1 activation signals or interferon-γ, M2 macrophages can express M1-specific cytokines and markers, thereby transforming to the M1 phenotype (Stout et al., 2005; Mylonas et al., 2009). Although there is no universal consensus on the transformation of microglial phenotype, phenotype changes in macrophages induced by external factors are dynamic and show heterogeneity in space and time. Consequently, the phenotypic definition of macrophages should be interpreted based on specific markers and function. As such, the real situation is by no means as simple as M1/M2.

Zhang et al. (2015) reported that TBI rats treated with bMSC exosomes had significantly stronger learning ability than those in other groups when tested using the Morris water maze at 34–35 days after injury. In addition, their sensory function and behavioral scores were higher than those of other groups at 14–35 days post-TBI. In the same study, the exosome treatment group also had significantly more neovascular endothelial cells in the dentate gyrus that effectively reduced neuroinflammation. This was the first *in vivo* study of exosomes and their role in the treatment of TBI. Herein, the damaged area in the TBI + Exo group was significantly less than that of the TBI and TBI + saline groups. In addition, the number of TUNEL-positive cells in the damaged area was also significantly reduced after treatment with exosomes. This strongly indicated that the use of exosomes in the acute phase after TBI could reduce brain tissue damage and cerebral cortical cells apoptosis. In the same line, the neuroinflammatory response in the exosome treatment group was inhibited. The expression of pro-inflammatory factors, IL-1β and TNF-α, was significantly suppressed while that of the anti-inflammatory factors, IL-10 and TGF-β, was significantly increased. The expression of the M2-type microglia marker, Arg1, was also significantly increased in the exosome treatment group.

There are numerous studies on neuroinflammation-related signal pathways. Cheng et al. (2019) reported that the expression of the Notch1/NFκB pathway protein was significantly higher in the cerebral ischemic stroke models. However, Zeng et al. (2017) reported that hypertonic saline attenuated the expression of pro-inflammatory mediators and downregulate the Notch signaling pathway. The role of the STAT3 signaling pathway during inflammation is controversial. Ryu et al. (2019) reported that dasatinib regulated the neuroinflammatory response of lipopolysaccharide-induced microglia and astrocytes by inhibiting the expression of STAT3 and pro-inflammatory factors. Similarly, Zhang et al. (2018) reported that ginkgo biloba extract protected brain tissues after ischemic stroke by significantly reducing the expression of pro-inflammatory cytokines. These effects may have been achieved by inhibiting the JAK2/STAT3 pathway. However, Staples reported that IL-10 activated the phosphorylation of transcription factor STAT3 through the autocrine feedback. As such, activation of STAT3 could upregulate the expression of IL-10. The autocrine feedback enhanced the anti-inflammatory effects of IL-10 (Staples et al., 2007).

The relationship between IL-10 and STAT3 seems to be particularly subtle. IL-10 plays a role in the anti-inflammatory response by binding to its receptor. The activation of the IL-10/JAK1/STAT3 cascade pathway in turn causes activation of phosphorylated STAT3 within seconds. Although STAT3 has no anti-inflammatory effects, it can activate many anti-inflammatory effector genes that can inhibit pro-inflammatory genes at the transcriptional level (Murray, 2005, 2006). Herein, the IL-10 level in the exosomes treatment group was significantly higher than that in the other two groups on days 1, 3, and 7 post-TBI. Moreover, the expression of STAT3 in the exosome treatment group was significantly higher than that in the TBI group on day 7 post-TBI. Based on the interaction between IL-10 and STAT3, it can be concluded that IL-10 activates the STAT3 cascade pathway to inhibit neuroinflammation and promote the transformation of microglia to an anti-inflammatory phenotype.

Recently, researchers have postulated that the therapeutic effect of exosomes depends on large amounts of microRNAs (Mateescu et al., 2017; Shao et al., 2017). microRNA sequencing was performed to measure the expression level of microRNAs in exosomes and bMSCs. Based on microRNAs reported in other relevant studies and the sequencing results, let-7c, miR-124, miR-21a, and miR-181b were screened to identify those strongly associated with neuroinflammation. Subsequent quantitative polymerase chain reaction results of the brain tissue revealed that the expression of miR-181b in the exosome treatment group was significantly higher than that in the other groups. It was thus concluded that miR-181b may be involved in the regulation of neuroinflammation, as well as regulation of the microglial phenotype.

Further investigations on the effects of miR-181b using lentiviral vectors revealed that there were significantly fewer apoptotic cells in the TBI-up group than in the other groups. The TBI-up group had significantly higher levels of IL-10 and TGF-β and lower levels of IL-1β and TNF-α than the TBI-

down and TBI groups. Further analysis revealed that the expression levels of IL-10 and TGF-β gradually increased after TBI. Compared with the TBI group, the expression levels of ARG1 and STAT3 in the TBI-up group were significantly higher, while the expression of iNOS was lower. Taken together, these results strongly suggested that there may be some interaction between the miR-181b and IL-10/STAT3 pathway. These effects could culminate with a phenotype transformation of microglia and inhibition of neuroinflammation and cell apoptosis.

This study was limited by several factors. The direct targets of miR181b and the mechanism of how miR-181b activates the IL-10/STAT3 pathway were not identified. Further studies on miR181b targets and their mechanisms of action are therefore needed to decipher its role in neuroprotection. Despite the limitation, our current study disclosed that exosomes derived from bMSCs can inhibit neuroinflammation both *in vitro* and *in vivo* as well as reducing apoptosis after TBI. microRNA-181b plays a role as a potential target that may regulate the IL-10/STST3 pathway and subsequently influence the neuroinflammation in some manner.

In conclusion, exosomes derived from bMSCs promote the polarization of microglia to the anti-inflammatory phenotype and inhibit the neuroinflammatory response both *in vitro* and *in vivo*. miR-181b seems to play a role in this process. The prominent role of microRNAs in neuroprotection offers new potential avenues of research into the treatment of neuroinflammation post-TBI.

Acknowledgments: *We gratefully acknowledge the kind cooperation of He Li (Alibaba Group, Hangzhou, China) in the statistical analysis of this research.*
Author contributions: *Study conception and design: LW, YDW, XFY; experiment implementation and data analysis: YDW, PDZ, MDT; experimental assistance: DFS, HW; manuscript draft: YDW; manuscript revision: WDY, YRZ, JFF. All authors read and approved the final manuscript.*
Conflicts of interest: *The authors declare that the research was conducted in the absence of any commercial or financial relationships that could be construed as a potential conflict of interest.*
Author statement: *This paper has been posted as a preprint on Research Square with doi: https://doi.org/10.21203/rs.3.rs-151671/v1, which is available from: https://assets.researchsquare.com/files/rs-151671/v1/c37419fc-bd38-4c8b-a4a3-49e04c4b7b59.pdf?c=1631871873.*
Availability of data and materials: *All data generated or analyzed during this study are included in this published article and its supplementary information files.*

Open peer reviewer: *Evguenia P Bekman, Universidade de Lisboa Instituto Superior Tecnico, Portugal.*
Additional file: *Open peer review report 1.*

References

Arnò B, Grassivaro F, Rossi C, Bergamaschi A, Castiglioni V, Furlan R, Greter M, Favaro R, Comi G, Becher B, Martino G, Muzio L (2014) Neural progenitor cells orchestrate microglia migration and positioning into the developing cortex. Nat Commun 5:5611.

Arslan F, Lai RC, Smeets MB, Akeroyd L, Choo A, Aguor EN, Timmers L, van Rijen HV, Doevendans PA, Pasterkamp G, Lim SK, de Kleijn DP (2013) Mesenchymal stem cell-derived exosomes increase ATP levels, decrease oxidative stress and activate PI3K/Akt pathway to enhance myocardial viability and prevent adverse remodeling after myocardial ischemia/reperfusion injury. Stem Cell Res 10:301-312.

Bian S, Zhang L, Duan L, Wang X, Min Y, Yu H (2014) Extracellular vesicles derived from human bone marrow mesenchymal stem cells promote angiogenesis in a rat myocardial infarction model. J Mol Med (Berl) 92:387-397.

Cheng M, Yang L, Dong Z, Wang M, Sun Y, Liu H, Wang X, Sai N, Huang G, Zhang X (2019) Folic acid deficiency enhanced microglial immune response via the Notch1/nuclear factor kappa B p65 pathway in hippocampus following rat brain I/R injury and BV2 cells. J Cell Mol Med 23:4795-4807.

Fesharaki M, Razavi S, Ghasemi-Mobarakeh L, Behjati M, Yarahmadian R, Kazemi M, Hejazi H (2018) Differentiation of human scalp adipose-derived mesenchymal stem cells into mature neural cells on electrospun nanofibrous scaffolds for nerve tissue engineering applications. Cell J 20:168-176.

Hansson E, Rönnbäck L (2003) Glial neuronal signaling in the central nervous system. FASEB J 17:341-348.

Harrison EB, Hochfelder CG, Lamberty BG, Meays BM, Morsey BM, Kelso ML, Fox HS, Yelamanchili SV (2016) Traumatic brain injury increases levels of miR-21 in extracellular vesicles: implications for neuroinflammation. FEBS Open Bio 6:835-846.

Hermann A, Gastl R, Liebau S, Popa MO, Fiedler J, Boehm BO, Maisel M, Lerche H, Schwarz J, Brenner R, Storch A (2004) Efficient generation of neural stem cell-like cells from adult human bone marrow stromal cells. J Cell Sci 117:4411-4422.

Huang H, Chen L, Mao G, Sharma HS (2020) Clinical neurorestorative cell therapies: developmental process, current state and future prospective. J Neurorestoratol 8:61-82.

Italiani P, Mazza EM, Lucchesi D, Cifola I, Gemelli C, Grande A, Battaglia C, Bicciato S, Boraschi D (2014) Transcriptomic profiling of the development of the inflammatory response in human monocytes in vitro. PLoS One 9:e87680.

Kigerl KA, Gensel JC, Ankeny DP, Alexander JK, Donnelly DJ, Popovich PG (2009) Identification of two distinct macrophage subsets with divergent effects causing either neurotoxicity or regeneration in the injured mouse spinal cord. J Neurosci 29:13435-13444.

Kim DK, Nishida H, An SY, Shetty AK, Bartosh TJ, Prockop DJ (2016) Chromatographically isolated CD63+CD81+ extracellular vesicles from mesenchymal stromal cells rescue cognitive impairments after TBI. Proc Natl Acad Sci U S A 113:170-175.

Kirkley KS, Popichak KA, Afzali MF, Legare ME, Tjalkens RB (2017) Microglia amplify inflammatory activation of astrocytes in manganese neurotoxicity. J Neuroinflammation 14:99.

Kumar A, Loane DJ (2012) Neuroinflammation after traumatic brain injury: opportunities for therapeutic intervention. Brain Behav Immun 26:1191-1201.

Lai RC, Arslan F, Lee MM, Sze NS, Choo A, Chen TS, Salto-Tellez M, Timmers L, Lee CN, El Oakley RM, Pasterkamp G, de Kleijn DP, Lim SK (2010) Exosome secreted by MSC reduces myocardial ischemia/reperfusion injury. Stem Cell Res 4:214-222.

Li Y, Yang YY, Ren JL, Xu F, Chen FM, Li A (2017) Exosomes secreted by stem cells from human exfoliated deciduous teeth contribute to functional recovery after traumatic brain injury by shifting microglia M1/M2 polarization in rats. Stem Cell Res Ther 8:198.

Liu MW, Huang YQ, Qu YP, Wang DM, Tang DY, Fang TW, Su MX, Wang YQ (2018) Protective effects of Panax notoginseng saponins in a rat model of severe acute pancreatitis occur through regulation of inflammatory pathway signaling by upregulation of miR-181b. Int J Immunopathol Pharmacol 32:2058738418818630.

Mateescu B, Kowal EJ, van Balkom BW, Bartel S, Bhattacharyya SN, Buzás EI, Buck AH, de Candia P, Chow FW, Das S, Driedonks TA, Fernández-Messina L, Haderk F, Hill AF, Jones JC, Van Keuren-Jensen KR, Lai CP, Lässer C, Liegro ID, Lunavat TR, et al. (2017) Obstacles and opportunities in the functional analysis of extracellular vesicle RNA- an ISEV position paper. J Extracell Vesicles 6:1286095.

Meng Y, Shang F, Zhu Y (2019) miR-124 participates in the proliferation and differentiation of brain glioma stem cells through regulating Nogo/NgR expression. Exp Ther Med 18:2783-2788.

Mosser CA, Baptista S, Arnoux I, Audinat E (2017) Microglia in CNS development: Shaping the brain for the future. Prog Neurobiol 149-150:1-20.

Murray PJ (2005) The primary mechanism of the IL-10-regulated antiinflammatory response is to selectively inhibit transcription. Proc Natl Acad Sci U S A 102:8686-8691.

Murray PJ (2006) Understanding and exploiting the endogenous interleukin-10/STAT3-mediated anti-inflammatory response. Curr Opin Pharmacol 6:379-386.

Mylonas KJ, Nair MG, Prieto-Lafuente L, Paape D, Allen JE (2009) Alternatively activated macrophages elicited by helminth infection can be reprogrammed to enable microbial killing. J Immunol 182:3084-3094.

Ni J, Wang X, Chen S, Liu H, Wang Y, Xu X, Cheng J, Jia J, Zhen X (2015) MicroRNA let-7c-5p protects against cerebral ischemia injury via mechanisms involving the inhibition of microglia activation. Brain Behav Immun 49:75-85.

Pettersen JS, Fuentes-Duculan J, Suárez-Fariñas M, Pierson KC, Pitts-Kiefer A, Fan L, Belkin DA, Wang CQ, Bhuvanendran S, Johnson-Huang LM, Bluth MJ, Krueger JG, Lowes MA, Carucci JA (2011) Tumor-associated macrophages in the cutaneous SCC microenvironment are heterogeneously activated. J Invest Dermatol 131:1322-1330.

Pirzad Jahromi G, Shabanzadeh Pirsaraei A, Sadr SS, Kaka G, Jafari M, Seidi S, Charish J (2015) Multipotent bone marrow stromal cell therapy promotes endogenous cell proliferation following ischemic stroke. Clin Exp Pharmacol Physiol 42:1158-1167.

Pozzo ED, Tremolanti C, Costa B, Giacomelli C, Milenkovic VM, Bader S, Wetzel CH, Rupprecht R, Taliani S, Settimo FD, Martini C (2019) Microglial pro-inflammatory and anti-inflammatory phenotypes are modulated by translocator protein activation. Int J Mol Sci 20:4467.

Qin C, Liu Q, Hu ZW, Zhou LQ, Shang K, Bosco DB, Wu LJ, Tian DS, Wang W (2018) Microglial TLR4-dependent autophagy induces ischemic white matter damage via STAT1/6 pathway. Theranostics 8:5434-5451.

Rager TM, Olson JK, Zhou Y, Wang Y, Besner GE (2016) Exosomes secreted from bone marrow-derived mesenchymal stem cells protect the intestines from experimental necrotizing enterocolitis. J Pediatr Surg 51:942-947.

Ransohoff RM, Schafer D, Vincent A, Blachère NE, Bar-Or A (2015) Neuroinflammation: ways in which the immune system affects the brain. Neurotherapeutics 12:896-909.

Reis LA, Borges FT, Simões MJ, Borges AA, Sinigaglia-Coimbra R, Schor N (2012) Bone marrow-derived mesenchymal stem cells repaired but did not prevent gentamicin-induced acute kidney injury through paracrine effects in rats. PLoS One 7:e44092.

Ryu KY, Lee HJ, Woo H, Kang RJ, Han KM, Park H, Lee SM, Lee JY, Jeong YJ, Nam HW, Nam Y, Hoe HS (2019) Dasatinib regulates LPS-induced microglial and astrocytic neuroinflammatory responses by inhibiting AKT/STAT3 signaling. J Neuroinflammation 16:190.

Shao L, Zhang Y, Lan B, Wang J, Zhang Z, Zhang L, Xiao P, Meng Q, Geng YJ, Yu XY, Li Y (2017) MiRNA-sequence indicates that mesenchymal stem cells and exosomes have similar mechanism to enhance cardiac repair. Biomed Res Int 2017:4150705.

Shevela E, Davydova M, Starostina N, Yankovskaya A, Ostanin A, Chernykh E (2019) Intranasal delivery of M2 macrophage-derived soluble products reduces neuropsychological deficit in patients with cerebrovascular disease: a pilot study. J Neurorestoratol 7:89-100.

Staples KJ, Smallie T, Williams LM, Foey A, Burke B, Foxwell BM, Ziegler-Heitbrock L (2007) IL-10 induces IL-10 in primary human monocyte-derived macrophages via the transcription factor Stat3. J Immunol 178:4779-4785.

Stout RD, Suttles J (2004) Functional plasticity of macrophages: reversible adaptation to changing microenvironments. J Leukoc Biol 76:509-513.

Stout RD, Jiang C, Matta B, Tietzel I, Watkins SK, Suttles J (2005) Macrophages sequentially change their functional phenotype in response to changes in microenvironmental influences. J Immunol 175:342-349.

Tan CY, Lai RC, Wong W, Dan YY, Lim SK, Ho HK (2014) Mesenchymal stem cell-derived exosomes promote hepatic regeneration in drug-induced liver injury models. Stem Cell Res Ther 5:76.

Tian T, Zhang HX, He CP, Fan S, Zhu YL, Qi C, Huang NP, Xiao ZD, Lu ZH, Tannous BA, Gao J (2018) Surface functionalized exosomes as targeted drug delivery vehicles for cerebral ischemia therapy. Biomaterials 150:137-149.

Timmers L, Lim SK, Arslan F, Armstrong JS, Hoefer IE, Doevendans PA, Piek JJ, El Oakley RM, Choo A, Lee CN, Pasterkamp G, de Kleijn DP (2007) Reduction of myocardial infarct size by human mesenchymal stem cell conditioned medium. Stem Cell Res 1:129-137.

van Koppen A, Joles JA, van Balkom BW, Lim SK, de Kleijn D, Giles RH, Verhaar MC (2012) Human embryonic mesenchymal stem cell-derived conditioned medium rescues kidney function in rats with established chronic kidney disease. PLoS One 7:e38746.

Vogel DY, Vereyken EJ, Glim JE, Heijnen PD, Moeton M, van der Valk P, Amor S, Teunissen CE, van Horssen J, Dijkstra CD (2013) Macrophages in inflammatory multiple sclerosis lesions have an intermediate activation status. J Neuroinflammation 10:35.

Wen L, You W, Wang Y, Zhu Y, Wang H, Yang X (2019) Investigating alterations in caecum microbiota after traumatic brain injury in mice. J Vis Exp:e59410.

Wislet-Gendebien S, Wautier F, Leprince P, Rogister B (2005) Astrocytic and neuronal fate of mesenchymal stem cells expressing nestin. Brain Res Bull 68:95-102.

Wong KL, Tai JJ, Wong WC, Han H, Sem X, Yeap WH, Kourilsky P, Wong SC (2011) Gene expression profiling reveals the defining features of the classical, intermediate, and nonclassical human monocyte subsets. Blood 118:e16-31.

Wood AM, Kaptoge S, Butterworth AS, Willeit P, Warnakula S, Bolton T, Paige E, Paul DS, Sweeting M, Burgess S, Bell S, Astle W, Stevens D, Koulman A, Selmer RM, Verschuren WMM, Sato S, Njølstad I, Woodward M, Salomaa V, et al. (2018) Risk thresholds for alcohol consumption: combined analysis of individual-participant data for 599 912 current drinkers in 83 prospective studies. Lancet 391:1513-1523.

Xin H, Li Y, Cui Y, Yang JJ, Zhang ZG, Chopp M (2013) Systemic administration of exosomes released from mesenchymal stromal cells promote functional recovery and neurovascular plasticity after stroke in rats. J Cereb Blood Flow Metab 33:1711-1715.

Xu C, Fu F, Li X, Zhang S (2017) Mesenchymal stem cells maintain the microenvironment of central nervous system by regulating the polarization of macrophages/microglia after traumatic brain injury. Int J Neurosci 127:1124-1135.

Zeng WX, Han YL, Zhu GF, Huang LQ, Deng YY, Wang QS, Jiang WQ, Wen MY, Han QP, Xie D, Zeng HK (2017) Hypertonic saline attenuates expression of Notch signaling and proinflammatory mediators in activated microglia in experimentally induced cerebral ischemia and hypoxic BV-2 microglia. BMC Neurosci 18:32.

Zhang SC, Fedoroff S (1996) Neuron-microglia interactions in vitro. Acta Neuropathol 91:385-395.

Zhang Y, Chopp M, Meng Y, Katakowski M, Xin H, Mahmood A, Xiong Y (2015) Effect of exosomes derived from multipluripotent mesenchymal stromal cells on functional recovery and neurovascular plasticity in rats after traumatic brain injury. J Neurosurg 122:856-867.

Zhang Y, Liu J, Yang B, Zheng Y, Yao M, Sun M, Xu L, Lin C, Chang D, Tian F (2018) Ginkgo biloba extract inhibits astrocytic lipocalin-2 expression and alleviates neuroinflammatory injury via the JAK2/STAT3 pathway after ischemic brain stroke. Front Pharmacol 9:518.

Zhao EY, Jia YJ, Wang DM, Wen GQ, Guan WJ, Jing LJ, Deng YD (2015) Effect of p65 gene inhibited by siRNA on differention of rat marrow mesenchymal stem cells into neurons. Zhongguo Ying Yong Sheng Li Xue Za Zhi 31:254-258.

Zhu YG, Feng XM, Abbott J, Fang XH, Hao Q, Monsel A, Qu JM, Matthay MA, Lee JW (2014) Human mesenchymal stem cell microvesicles for treatment of Escherichia coli endotoxin-induced acute lung injury in mice. Stem Cells 32:116-125.

Zhuang X, Xiang X, Grizzle W, Sun D, Zhang S, Axtell RC, Ju S, Mu J, Zhang L, Steinman L, Miller D, Zhang HG (2011) Treatment of brain inflammatory diseases by delivering exosome encapsulated anti-inflammatory drugs from the nasal region to the brain. Mol Ther 19:1769-1779.

P-Reviewer: Bekman EP; C-Editor: Zhao M; S-Editors: Yu J, Li CH; L-Editors: Yu J, Song LP; T-Editor: Jia Y